Drought and Moisture Availability and Recent Western Spruce Budworm Outbreaks in the Western United States

A Thesis
Presented in Partial Fulfillment of the Requirements for the
Degree of Master of Science
with a
Major in Environmental Science
in the
College of Graduate Studies
University of Idaho
by

Bingbing Xu

Major Professor: Jeffrey Hicke, Ph.D.
Committee Members: John Abatzoglou, Ph.D.; Lee Vierling, Ph.D.
Department Administrator: J.D. Wulfhorst, Ph.D.

December 2018

Authorization to Submit Thesis

This thesis of Bingbing Xu, submitted for the degree of Master of Science with a Major in Environmental Science and titled, “Drought and Moisture Availability and Recent Western Spruce Budworm Outbreaks in the Western United States,” has been reviewed in final form. Permission, as indicated by the signatures and dates below, is now granted to submit final copies to the College of Graduate Studies for approval.

Major Professor: _____ Date _____

Jeffrey Hicke, Ph.D.

Committee Members: _____ Date _____

John Abatzoglou, Ph.D.

_____ Date _____

Lee Vierling, Ph.D.

Department Administrator: _____ Date _____

J.D. Wulfhorst, Ph.D.

Abstract

Western spruce budworm (WSBW) is a common defoliating insect that has caused extensive damage to a number of tree species across the western United States (US). Past studies have linked outbreaks of WSBW to increases of moisture stress of host trees in Northwest US and decreased moisture stress in Southwest US. This study analyzed seasonal drought stress metrics in multiple locations with WSBW outbreaks in the western US during 1997-2015 identified from aerial detection surveys. Superposed epoch analysis and insect population growth rates (as represented by defoliation area change) were assessed to quantify the drought condition associated with the initiation and continuation of outbreaks, respectively. We found that a few consecutive years of drought were associated with outbreak initiation in the Northwest US, but that outbreak initiation of the Southwest US was associated with only weak drought or neutral conditions. During outbreak continuation stage, there was a weak correlation between the increase of May moisture availability and insect population increase in the Southwest, and no apparent correlation in the Northwest. Given future climate change, the increase of summer drought frequency may increase WSBW outbreaks, and thus improved understanding of the role of drought, as presented here, will lead to improved predictions and management of future outbreaks of WSBW.

Acknowledgments

Firstly, I would like to thank my advisor, Dr. Jeffrey Hicke, who generously offer his expertise and guidance to my research and professional development. Dr. Hicke helps me with remote sensing and climate data acquisition, refining proper statistical analysis method, and developing code for data processing. I am grateful for Dr. John Abatzoglou, who provided part of the climate data used in this thesis, and also helped with the interpretation of climate data. Thank you to Dr. Lee Vierling, who offered me advice and insight on refining study region and other aspects of my research.

This study was supported by funds from the Glacier National Park Foundation, and the teaching assistantship from Environmental Science program of the College of Natural Resource at the University of Idaho.

Dedication

To my parents and my husband,
thank you for your support and encouragement.

Table of Contents

List of Figures

1. Introduction

1.1. Ecology of western spruce budworm

Western spruce budworm (*Choristoneura freemani*, WSBW) is a common and destructive defoliating insect of western North America. It feeds on many spruce and fir species, including widespread species such as Douglas-fir (*Pseudotsuga menziesii*) and subalpine fir (*Abies lasiocarpa*). The host species of WSBW can be found in most states of the western US, and WSBW distribution overlaps with most of its hosts' ranges.

WSBW usually completes one life cycle per year. Adults emerge from pupae and lay eggs in late July or early August. Larvae hatch from eggs in about ten days and find overwintering sites without feeding, and in late April and May of the next year, larvae emerge from hibernacula and start feeding (Fellin and Dewey 1982). WSBW larvae feed on foliage, preferably new foliage, staminate flowers, and developing cones of its host species. While feeding, larvae leave webs that entangle and cover developing foliage (Fellin and Dewey 1982). These webs can reduce photosynthesis, and needles can turn red if defoliation persists (Fellin and Dewey 1982). The red color or bare top of a tree is used as an indicator of WSBW presence during aerial detection surveys of tree damage (Fellin and Dewey 1982). Reduction of foliage slows the growth of the host tree, and prolonged disturbance may cause top-kill or even mortality and damage to developing cones and flowers, which influences the reproduction of trees and inhibits recovery of attacked trees (Fellin and Dewey 1982). WSBW thrive in stands with multiple canopy layers: at high populations, or due to physical disturbances, larvae may fall from upper canopy layers, and if they land on host species, they can continue to feed and cause more damage (Campbell 1993).

Outbreaks are considered cyclical and can occur synchronously across broad spatial scale (e.g., Flower 2016). Outbreaks return every 25 to 37 years, but many factors, including local temperature and moisture conditions, determine the exact timing and severity of an outbreak (Ryerson et al. 2003, Flower 2016).

1.2 Climate and WSBW relationships

Moisture-caused stress of host trees is thought to be important for influencing a WSBW outbreak. A hump-shaped relationship between moisture stress and WSBW larvae survival rate has been suggested, in which intermittent moisture stress is most beneficial for outbreaks (Campbell 1993, Huberty and Denno 2004). Compared to an unstressed host, a stressed host has altered foliage qualities such as increased nitrogen and carbohydrates content and reduced moisture availability (White 1984, Mattson and Haack 1987, Campbell 1993, Parks 1993). Moisture-stressed plants break down nitrogen, a limiting factor of the larvae, to soluble forms, and larvae that feed on these plants are more successful because of this better supply of nitrogen (White 1984, Mattson and Haack 1987). Experiments suggest that the peak of larvae feeding activity also matches the carbohydrate level of the stressed host, implying that moisture-stressed hosts encourage feeding by larvae (Mattson and Haack 1987). Laboratory experiments also reveal that compared with larvae feeding on normal plants, larvae feeding on moisture-stressed plants grow faster and have greater survival rate (Parks 1993).

Severe and prolonged drought, however, may be detrimental to WSBW (Mattson and Haack 1987, Campbell 1993). Severely stressed hosts produce less and tougher foliage due to decreased water availability and photosynthesis, thus reducing food quality and quantity available to WSBW larvae (Mattson and Haack 1987). Extremely stressed trees also have a very high level of nitrogen, which reduced the survival rate of WSBW feeding on it (Brewer et al. 1985).

Moisture availability has been linked to WSBW outbreaks in observational studies that used satellite remote sensing and aerial surveys (Hard et al. 1980, Thomson et al. 1984, Senf et al. 2016) as well as dendrochronological reconstructions (Swetnam and Lynch 1993, Flower et al. 2014, Flower 2016). Spatially explicit methods that used aerial detection surveys (Hard et al. 1980, Thomson et al. 1984) or satellite imagery (Senf et al. 2016) have been used to analyze WSBW defoliations in southern British Columbia and the western US. Such methods have advantages of broader spatial extent but are often more limited in temporal extent. Dendrochronological data were used to analyze outbreaks over multiple centuries in multiple regions of North America, from British Columbia (Thomson and Benton 2007, Flower et al. 2014, Flower 2016) to New Mexico (Swetnam and Lynch 1993, Flower 2016).

Such studies are valuable for assessing climate influences over longer time periods but are often limited to a few locations (though see Flower (2016) for comparisons across western North America).

These empirical studies reveal that outbreaks in northern regions are associated with drought before initiation, whereas decreased moisture stress in the Southwest US leads to outbreaks. This major difference is associated with the mean climate in these locations: in the Southwest forests (New Mexico), climate conditions are more arid, and thus trees there are typically under more moisture stress. According to the plant vigor hypothesis, increased precipitation in this region could benefit outbreaks by providing more abundant food for WSBW (Price 1991).

Long-term analyses suggested that average moisture stress levels after outbreaks began to promote the continuation of outbreaks and prolonged drought reduce outbreaks (Flower et al. 2014, Flower 2016). Intermittent moisture stress levels allow budworm larvae to benefit from drought-induced host chemical change while not significantly impacting growth. These patterns support the pulsed plant stress hypothesis, which states that intermittent stress is the most suitable condition for herbivorous insects (Huberty and Denno 2004).

Thus, past studies have indicated some influences of drought on outbreaks of western spruce budworm, but with some variability. Given future climate change and effects on droughts (Wuebbles et al. 2017), additional studies that test and refine relationships to insect outbreaks will increase scientific understanding and forest management.

In this study, I compared drought patterns immediately preceding and during multiple outbreaks of WSBW across a wide area of the western US in recent years. I used aerial survey data, which allowed better identification of initiation year than dendrochronological data in past studies and provides coverage across a broad geographical extent. I employed multiple drought metrics from gridded climate data sets, including the commonly used Palmer Drought Severity Index (PDSI) as well as precipitation and climatic water deficit (CWD), a metric that may represent host stress better than PDSI or precipitation. I explored differences between drought influences on outbreaks in the Northwest versus Southwest US to assess possible variability in influences in regions with different climates. I considered both outbreak initiation (through the use of superposed epoch analyses) as well as outbreak continuation (though the analyses of insect population growth rate as represented by defoliation area).

2. Methods

2.1 Study regions

I selected ten study regions affected by WSBW in the western United States within the range of an important host species, Douglas-fir. These regions had high defoliation area for multiple years with typically complete survey coverage (see Section 2.2 for more details). I also ensured that region boundaries were defined to encompass the entire (local) area of an outbreak and that the outbreak dynamics within these regions were not influenced by insect dispersal from neighboring areas. Regions were selected to be representative of the wide geographic range of the host species range in the western US. Locations with outbreaks that initiated after the year when westwide aerial surveys data (ADS) became available (1997) were favored during selection to allow determination of the initiation year of an outbreak.

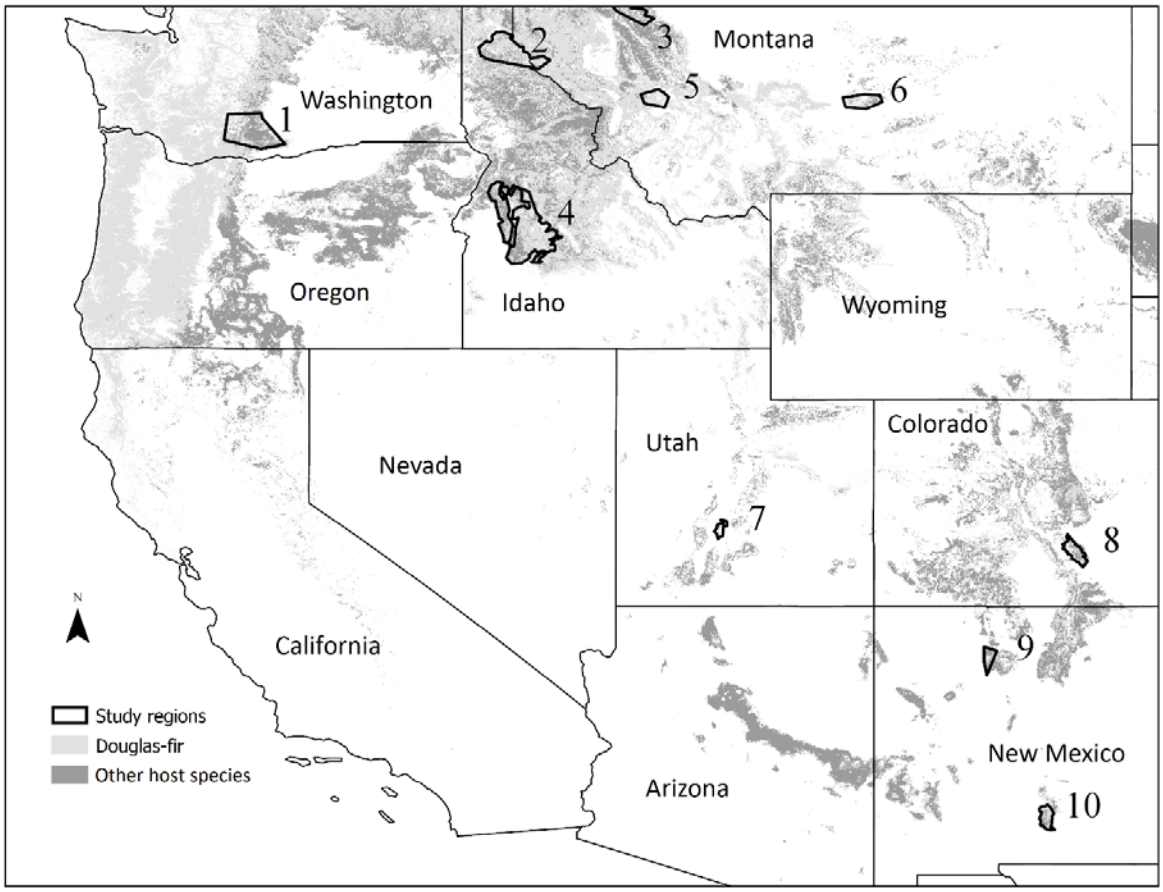

Figure 2.1. Ranges of host tree species of western spruce budworm (gray shading) and regions analyzed in this study (polygons and numbers).

2.2 Data sources

Defoliation caused by WSBW was identified from ADS data, which are annual surveys of forested areas of the United States. ADS data from 1997 to 2015 were acquired from the Insect & Disease Detection Survey Data Explorer (https://foresthealth.fs.usda.gov/portal/Flex/IDS). Except for Region 3, all regions were completely surveyed (flown) every year. Region 3 was surveyed after 2003 (and before an outbreak began), and in 2013 and 2015 had less than 50% coverage (when areas not flown were mostly unforested areas). Defoliated polygons were selected with the damage causal agent attribute, which identifies locations defoliated by WSBW. The severity attribute, which has values of 0 (no defoliation), 1 (low severity; 0-50% of a polygon was defoliated), or 2

(high severity; >50% defoliated), was used to adjust the defoliation area of each polygon to represent the influence of different degrees of defoliation better (see Section 2.3 for more information). If the pattern attribute of a polygon is labeled “continuous,” the polygon does not contain gaps of trees that are not damaged. Because most of the defoliation polygons within the selected regions were labeled “continuous,” the area of the defoliated polygon is likely an accurate representation of the defoliated area. Details about data attributes used in this study are described in Appendix B.

I considered multiple gridded climate data sets for use in this study. I used the TerraClimate dataset (Abatzoglou et al. 2018) (https://climate.northwestknowledge.net/TERRACLIMATE/index_directDownloads.php) because PDSI and CWD are included as variables. PDSI and CWD were considered here because including both temperature and moisture from current and past months in the calculations of a moisture stress metric can result in a better representation of host tree stress than other climate variables such as temperature or precipitation alone. TerraClimate was developed using high spatial resolution climatological normals of temperature and precipitation from the WorldClim dataset (Hijmans et al. 2005, Fick and Hijmans 2017) together with temporally varying data sets that include Climate Research Unit data (CRU Ts4.0) (Harris et al. 2014) and the Japanese 55-year Reanalysis (JRA-55) (Kobayashi et al. 2015). The CRU and JRA-55 data, which are at coarse spatial resolution, were downscaled with the WorldClim data. TerraClimate data are available at relatively high spatial resolution (4 km) and from 1958-2017. Potential evapotranspiration (PET) was calculated with the Penman Montieth approach (Abatzoglou et al. 2018). A one-dimensional modified Thornthwaite-Mather climatic water balance model was used to compute actual evapotranspiration (AET) and soil moisture, which were used in the calculations of PDSI and CWD (Palmer 1965, Abatzoglou et al. 2018). CWD is defined as the difference between PET and AET.

In addition to PDSI and CWD, precipitation was used to assess climatological mean moisture stress as well as in the analysis of insect population change. The Parameter-elevation Relationships on Independent Slopes Model version LT81 (PRISM) data set was chosen to provide precipitation information because it has finer spatial resolution (800 m). PRISM data was produced from a model developed by Daly et al. (2008) with topographic information and

weather station data (http://prism.oregonstate.edu/). This dataset was available from 1896 to 2018.

Monthly temperature from Topography Weather (TopoWX) was used to represent the range of climatological mean temperature among regions. TopoWX has a spatial resolution of 800 m and is available from 1948 to 2016 (http://www.scrimhub.org/resources/topowx/). TopoWX used data sources similar to PRISM, with the addition of remotely sensed MODIS land skin temperature to improve temperature accuracy, and slightly different spatial interpolation methods (Oyler et al. 2015a, Oyler et al. 2015b, Oyler et al. 2016).

2.3 Data processing and analysis

The area of defoliation from ADS data was used to represent defoliation damage and budworm populations. I calculated an index of damage that considers both defoliation area and severity. The adjusted total defoliation area of region *r* in year *y, ADS(r,y),* was calculated as:

$$ADS(r,y) = 0.25 * \sum_{p_{low}=1}^{Np_{low}(r)} DA_{low}(p_{low},y) + 0.75 * \sum_{p_{high}=1}^{Np_{high}(r)} DA_{high}(p_{high},y) \quad (2.1)$$

$DA_{low}(r,y)$ is the defoliation area of a low-severity polygon and DA_{high} is the defoliation area of a high-severity polygon. p_{high} is the number of high-severity polygons in region *r*, and p_{low} is the number of low-severity polygons in that region.

I defined outbreak initiation year and continuation years for each region using these defoliation time series. I defined the defoliation initiation year as the year when the adjusted defoliation area increased to greater than 80 hectares. Continuation years were defined as when the adjusted defoliation area of the previous year and current year were both greater than 80 hectares.

Moisture information from grid cells within the region was averaged to produce one annual time series. Water year and seasonal time series of precipitation, CWD, and PDSI were created for each area to assess seasonal influences on the relationship between drought metrics and WSBW outbreaks. To improve comparisons across regions, temporal anomalies

of CWD and precipitation were standardized to have a mean of 0 and a standard deviation of 1 using the 1960-2015 period as a baseline. PDSI was not adjusted since it is already adapted to local conditions (Palmer 1965, Abatzoglou et al. 2018).

Superposed epoch analysis (SEA) has been used when analyzing climate and defoliation time series (Flower et al. 2014, Flower 2016). For this study, SEA was used to assess the relationship between outbreak initiation and moisture stress of the host trees. SEA shifts each region's climate time series so that outbreak initiation years are aligned, then computes the mean climate time series across the regions. Time series from individual regions used in the SEA were inspected to ensure that the mean was not strongly influenced by highly anomalous regions. Confidence intervals were produced by bootstrapping the climate data of each region from 1960-2015 using 1000 samples. Data from the Northwest US (NW, five regions: Region 2-6), and Southwest (SW, three regions: Region 7, 8 and 10) were analyzed separately to ascertain any difference.

To study the relationship between defoliation area and moisture during the continuation stage, growth rates of insect populations were calculated and analyzed with different climate metrics. Like many organisms, changes in insect populations, not the populations themselves, respond to climate or other influences (Turchin 2003). Population dynamics are often represented by an exponential function, which leads to growth rates being represented by the current year population relative to the population in the previous year (Turchin 2003). I used the adjusted defoliation area as an indicator of the WSBW population. The annual growth rate was calculated with the formula

$$R(y) = \ln\left(\frac{ADA(y)}{ADA(y-1)}\right) \tag{2.2}$$

In this formula, *R(y)* is the growth rate in year *y*, *ADA(y)* is the adjusted defoliation area, and *ADA(y-1)* is the adjusted defoliation area in the previous year.

Plots of *R* versus anomalies of moisture stress illustrate growth rate responses to conditions wetter or drier than normal. In addition to computing linear regressions and associated R^2 values, plots were visually inspected to identify patterns. To represent the influence of recent precipitation on the growth condition of host plants at the beginning of the growing season, precipitation in May were included in this analysis in addition to PDSI and CWD. March and

April precipitation was excluded because the average temperature of March was too low for plant growth, and the moisture availability of April might be influenced by snowpack, which is not reflected by April precipitation (Figure 3.3).

I attempted to use multivariate analysis to explore climate/outbreak relationships. However, due to data constraints, the attempt was not very successful. See Appendix A for details.

3. Results

3.1 Characteristics of the study regions

Adjusted defoliation areas in the selected regions indicated outbreaks of western spruce budworm at different times for different regions throughout the study period (Figure 3.1). Outbreaks were in progress at the beginning of the survey period (Regions 1, 9), began and ended within the period (Region 2), or began and continued through the end of the survey period. Outbreak length was 6-7 years or longer in each region, with some regions having substantial defoliation for almost a decade. These time series were analyzed to find the initiation year for outbreaks of each region. Because Regions 1 and 9 had defoliation that was greater than 80 hectares at the beginning of the ADS time series (1997), their initiation year could not be identified. Defoliation initiation years ranged from 2002 to 2010. Region 4 (2002) had the earliest initiation year, while Region 8 had the latest initiation year (2010). Except for Region 4 and Region 2, most regions had initiation years after 2005.

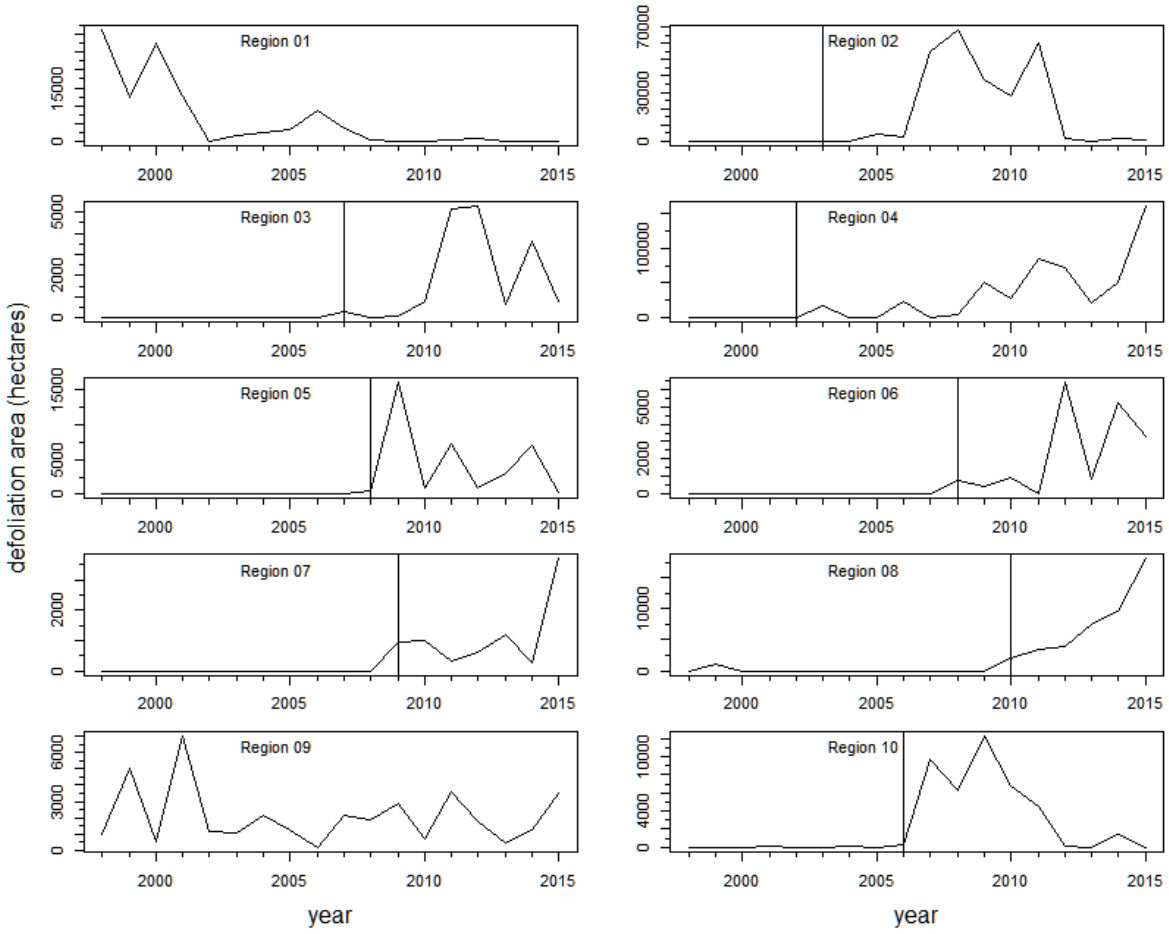

Figure 3.1. Adjusted defoliation area (ha) time series of regions used in the study. Vertical black lines indicate the initiation year used in the superposed epoch analysis. Because an outbreak was already ongoing in the first year of defoliation data (1997), Regions 1 (Washington) and 9 (Northern New Mexico) do not have initiation years.

Water-year mean temperature and the water-year total precipitation averaged across the study period (1997–2015) was calculated to show the general climate condition of each region (Figure 3.2). Generally, regions in the Northwest were wetter (434–1588 mm per year) than the Southwest (319–930 mm per year). Region 5 (434–708 mm per year), was an exception: it is in the Northwest and also the driest region. Temperatures ranged from 3.3 °C to 8.2 °C in the Northwest, and 4.0 °C to 9.9 °C in the Southwest. Region 10 was the warmest region (8.2–9.9 °C), due in part to its southernmost location.

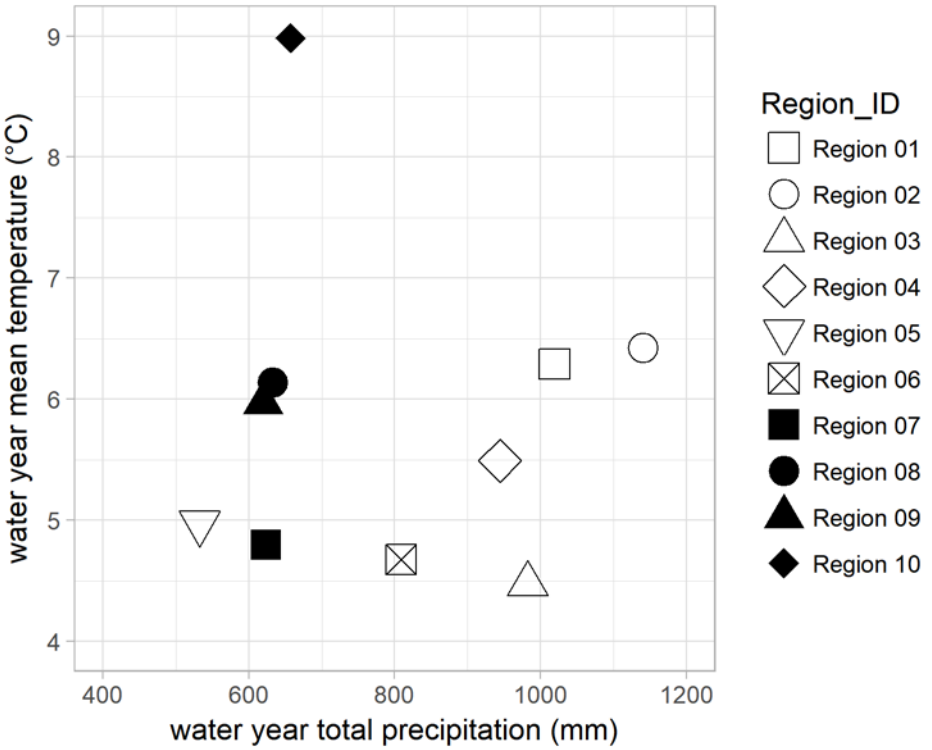

Figure 3.2. Average water-year total precipitation versus average water-year temperature of each study region. Hollow symbols are for regions in the Northwest, and solid symbols are for regions in the Southwest. Error bars indicate the range of water-year climate of each region.

I analyzed the average monthly climate of the Northwest and Southwest regions to assess moisture and temperature variations within a year (Figure 3.3). Temperatures in the Southwest were slightly higher than in the Northwest, except in July and August. A key difference between regions in the Northwest and Southwest is precipitation and its annual cycle. The Northwest had substantially higher precipitation from January to June, and from October to December, often twice as much. In July through September, regions in the Southwest had higher precipitation because of the monsoon moisture in the Southwest and the typically dry summers in the Northwest. CWD and PDSI annual cycles reflected these seasonal patterns of temperature and precipitation. Northwest PDSI was highest (indicating wettest conditions) in June, and then decreased until October. PDSI in the Southwest was low until June, then increased until October. In regions in the Northwest, CWD was elevated only June-September, with peaks in July and August. In contrast, Southwest CWD was relatively higher throughout most of the year, most notably during late spring and early summer before

monsoon rains came. The mean water year total CWD was 359 mm in the Northwest and the 638 mm in the Southwest.

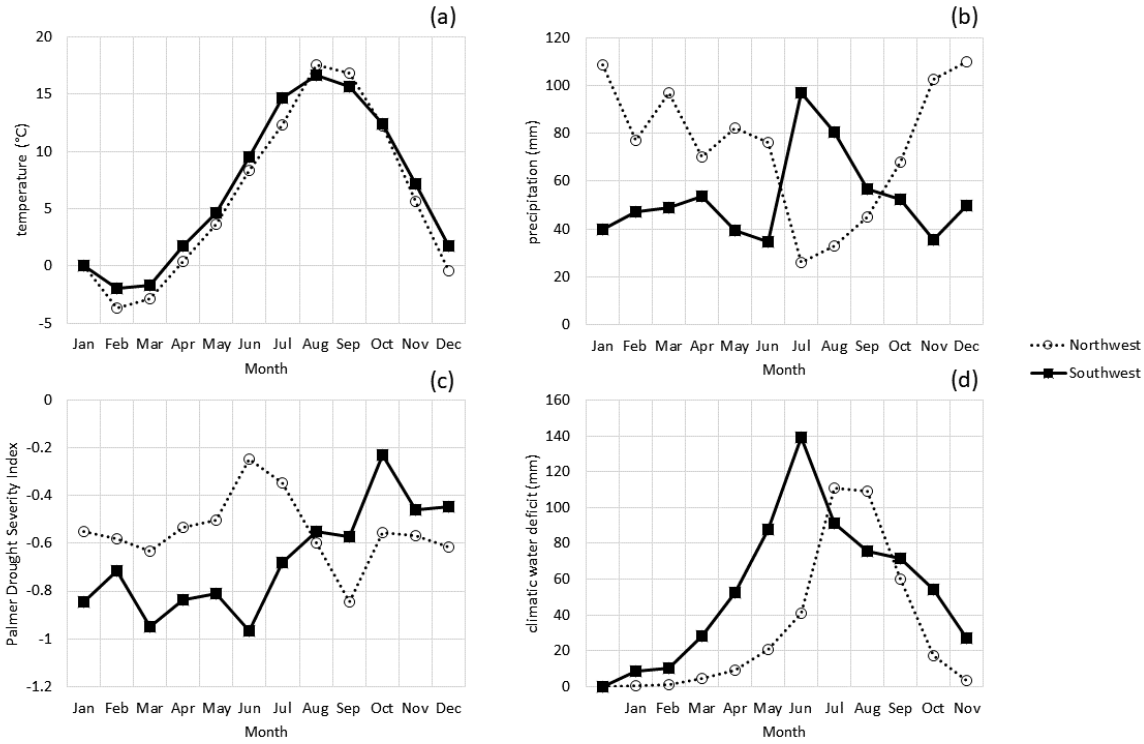

Figure 3.3. Average monthly climate of the Northwest and Southwest regions from 1997 to 2015. (a) temperature, (b) precipitation, (c) Palmer Drought Severity Index, and (d) climatic water deficit. Circles and dotted lines represent average climate metrics of Northwest regions, and squares and solid lines represent average climate metrics of Southwest regions.

3.2 Superposed epoch analysis

To assess the role of drought and moisture during outbreak initiation, I compared superposed epoch analyses using different moisture indices. Summer PDSI in the Northwest (five regions) was very low in the year of outbreak initiation (Figure 3.4a, statistically significantly different from 0 at the 90% level), and was low in the four years prior to initiation, particularly two years prior (also significant at the 90% level). For the Southwest (three regions), the role of drought was less clear: PDSI was slightly negative in the year of initiation and for a few of the prior years, but not in the year before initiation (Figure 3.4b).

Water-year and other seasonal PDSI metrics showed similar results (Appendix C, Appendix D, Appendix E, Appendix F).

A similar though somewhat stronger pattern occurred for CWD (Figure 3.5). For the Northwest, summer CWD was above the 1960-2015 average in the initiation year and the two years prior, with the year of initiation and year before statistically significantly different from 0 at the 95% level (Figure 3.5a, Appendix M). In the Southwest, CWD in the year of initiation was slightly negative (wetter) than average, with slightly drier years in earlier years (Figure 3.5b). Water-year CWD showed a similar trend compared to summer CWD, and other seasonal CWD analyses did not show strong responses (Appendix G, Appendix H, Appendix I, Appendix J)

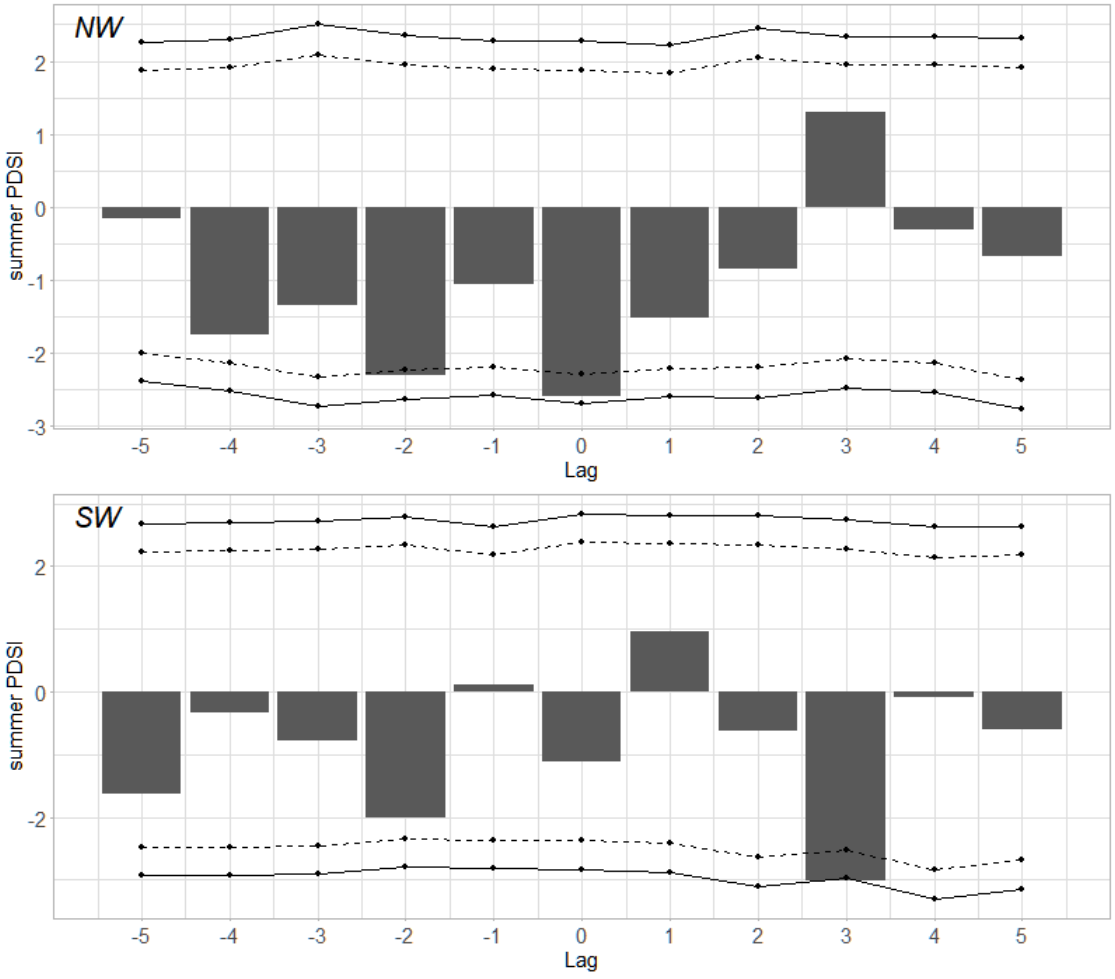

Figure 3.4. Superposed epoch analysis of summer Palmer Drought Severity Index. Dotted lines indicate 90% confidence intervals, and solid lines indicate 95% confidence intervals.

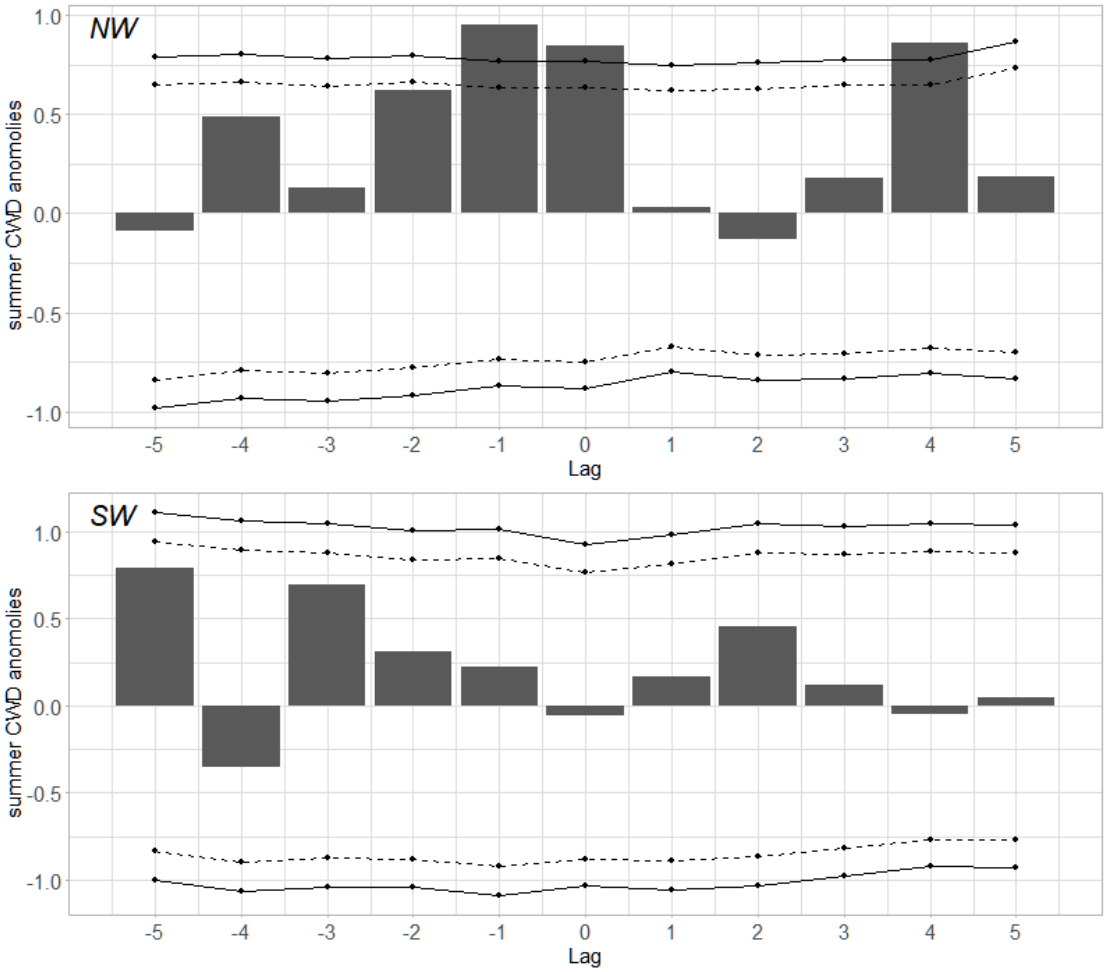

Figure 3.5. Superposed epoch analysis of summer standardized anomalies of climatic water deficit. Dotted lines indicate 90% confidence intervals, and solid lines indicate 95% confidence intervals.

3.3 Growth rate versus climate

Insect population growth rates exhibited only weak relationships to drought or moisture metrics. In spring, growth rates of the Southwest showed a weak correlation with May moisture indices, and the correlation with CWD was the strongest among these (R^2=0.12; Figure 3.6, Appendix K, Appendix L). During years with below-average CWD (indicting less stress), the number of years and regions with positive growth rates exceeded the number of years with negative growth rates. This pattern also supports the positive relationship between

wetter conditions and population increases. Summer PDSI showed a very weak negative correlation with the growth rate of the Northwest, while the Southwest showed no apparent relationship (Figure 3.7). Analyses of other seasonal and water-year PDSI and CWD also resulted in weak correlations, such as summer CWD (Figure 3.8). These findings are confirmed by inspecting the superposed epoch analyses (Figure 3.4, Figure 3.5) in the years following outbreak initiation, which reveals a mixture of weakly wet and dry years.

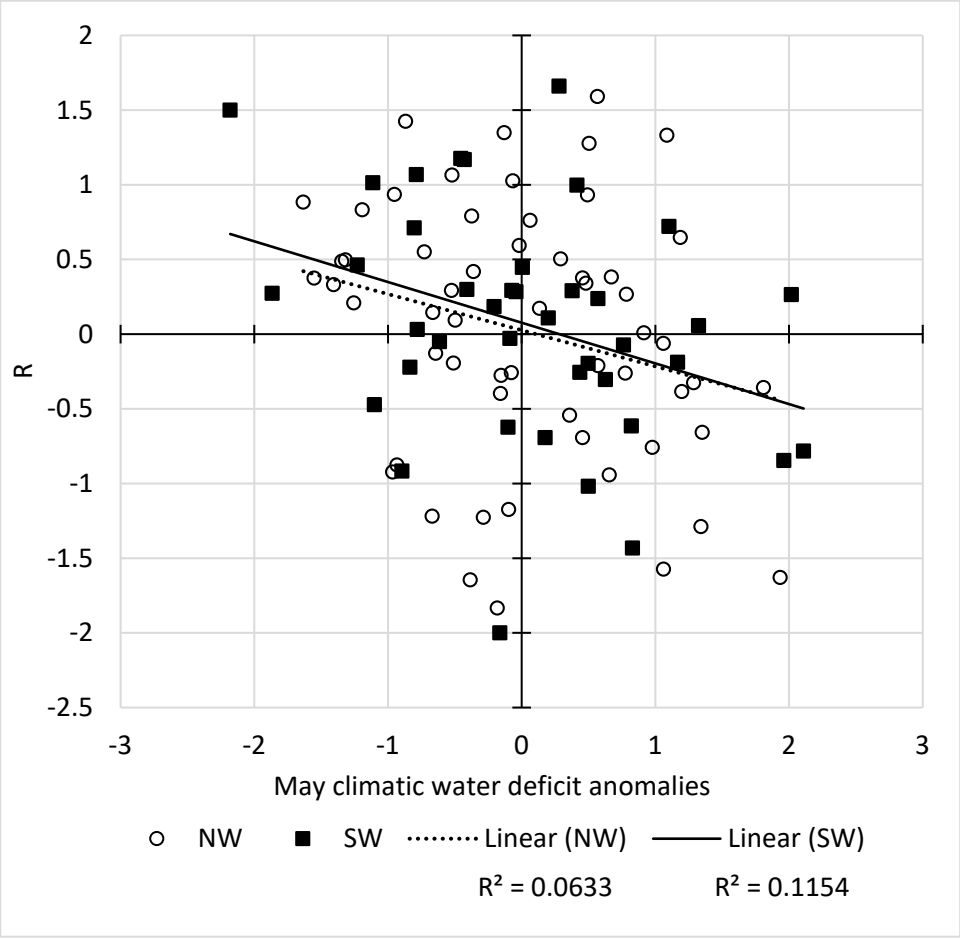

Figure 3.6. Western spruce budworm population growth rate (calculated using adjusted defoliation area from aerial surveys) versus standardized anomalies of May climatic water deficit. Solid squares indicate data from years and regions in the Southwest, and hollow circles indicate data from years and regions in the Northwest. The solid line is the trend line of data from Southwest regions, and the dotted line is the trend line of data from Northwest regions.

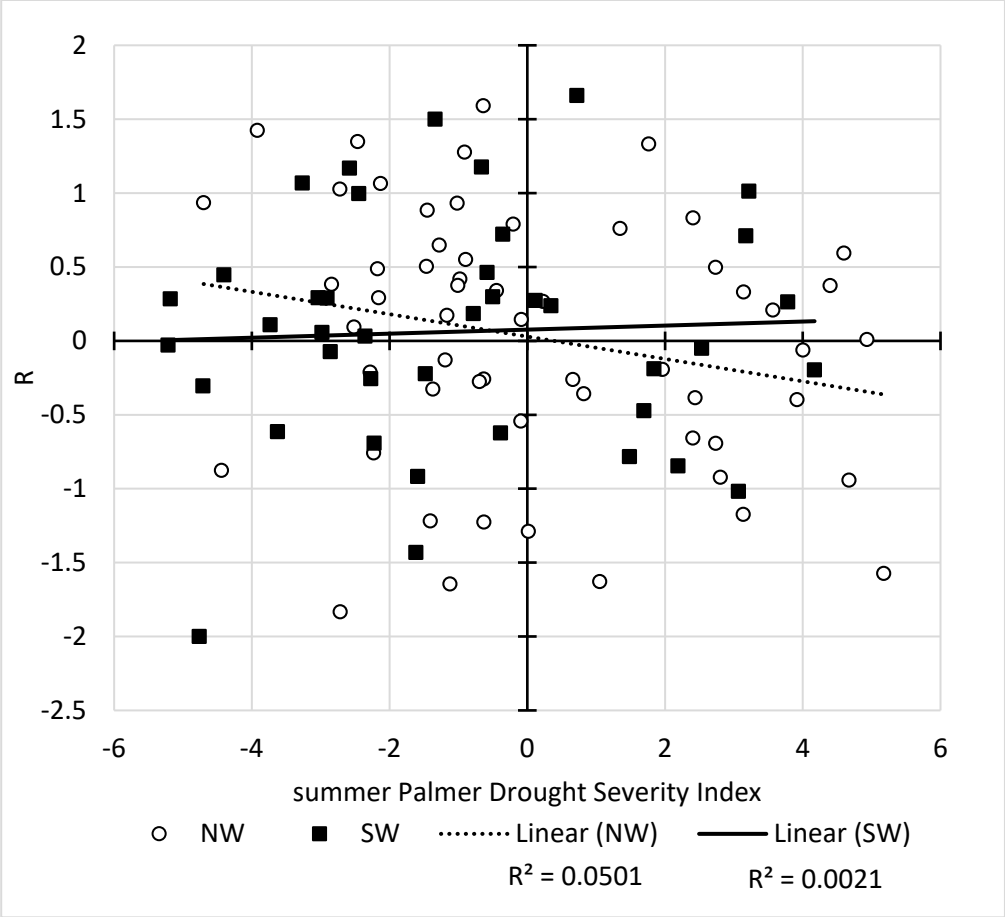

Figure 3.7. Western spruce budworm population growth rate (calculated using adjusted defoliation area from aerial surveys) versus summer Palmer Drought Severity Index. Solid squares indicate data from years and regions in the Southwest, and hollow circles indicate data from years and regions in the Northwest. The solid line is the trend line of data from Southwest regions, and the dotted line is the trend line of data from Northwest regions.

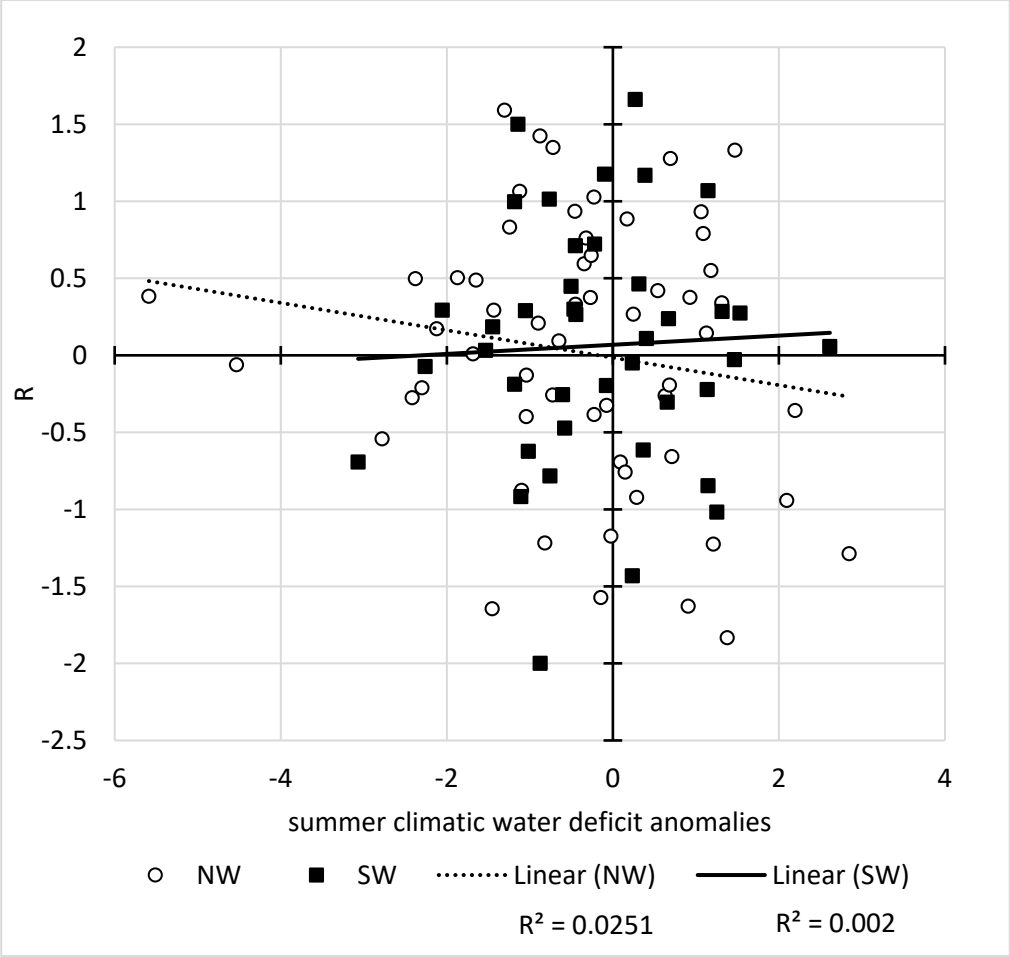

Figure 3.8. Western spruce budworm population growth rate (calculated using adjusted defoliation area from aerial surveys) versus summer of climatic water deficit. Solid squares indicate data from years and regions in the Southwest, and hollow circles indicate data from years and regions in the Northwest. The solid line is the trend line of data from Southwest regions, and the dotted line is the trend line of data from Northwest regions.

4. Discussion

The role of drought in initiating outbreaks of western spruce budworm varied from the Northwest to the Southwest. In regions of the Northwest, relatively dry conditions were present for several years before outbreaks and during the initiation year. Unlike the apparent role of drought in the initiation, population growth rates did not show any apparent relationship between moisture and outbreak continuation in the Northwest. In contrast, outbreak initiations in the Southwest were associated with weaker dry conditions, or neutral/wet conditions, compared with the Northwest. During the continuation stage, May moisture availability was slightly correlated with the increase of insect population, suggesting that the continuation stage of an outbreak may benefit from reduced moisture stress; other seasonal moisture metrics showed no correlation.

The influence of drought in the Northwest agrees with multiple previous studies of these insects in the same geographic area, which reported that drier conditions and moisture stress were beneficial for the initiation of outbreaks (Thomson et al. 1984, Flower et al. 2014, Flower 2016). This pattern may be explained by the change in foliage chemical composition when host trees are stressed. The increase in soluble nitrogen may benefit larvae by providing them with more of a limiting nutrient. Increases in carbohydrate content were suggested to stimulate feeding activities of larvae (Mattson and Haack 1987). The lack of drought signal during the continuation stage may have been caused by other factors that influence WSWB populations, which masked any relationship between growth rate and climate. These other factors include conspecific competition, dispersal, and predation, and are very challenging to represent given the scales of interest and available data in this study.

The role of drought in the Southwest has been reported by previous studies conducted in Colorado and New Mexico (Swetnam and Lynch 1993, Ryerson et al. 2003). These studies found that for relatively dry regions, where host species were constantly stressed, alleviating the moisture stress might lead to WSBW outbreaks (Swetnam and Lynch 1993, Ryerson et al. 2003). This might be explained by the bud condition change related to moisture stress. When the host trees are under moisture stress, they produce less foliage (Gower et al. 1992). Experiments performed on ponderosa pine (*Pinus ponderosa*), a host species of WSBW, indicated that trees would grow tougher foliage under moisture stress (McMillin and Wagner

1996). Those harder buds are difficult for the larvae to excavate, and the amount of foliage might not be enough to support large WSBW population. When moisture stress is alleviated, WSBW larvae have better and more abundant food resource, facilitating an increase of budworm populations. April and May in the Southwest are likely to be the beginning of growing season since the mean monthly temperatures of these months were above 0 ºC (Figure 3.3). In the Southwest, dry conditions occur on average during March to July, resulting in lower PDSI and higher CWD than other months. Thus, the moisture availability at the beginning of growing season in the Southwest should be relatively low. In this case, the increase of precipitation may allow trees to allocate more carbon to the aboveground portion, thus provide more food to the newly emerged budworm larvae, and increase their survival rate (Nealis and Régnière 2009).

Comparisons of climate variables indicate why drought plays a role in the Northwest but not in the Southwest. Regions in the Southwest are drier in terms of annual precipitation (Figure 3.2) and, importantly, are different in terms of the seasonal cycle of moisture stress (Figure 3.3). Winter and spring precipitation are substantially reduced in the Southwest compared with the Northwest, and temperatures are higher through June. Inspection of the seasonal cycle of temperatures suggests that the growing season begins in April or May in both the Southwest and Northwest. CWD is much higher during this period in the Southwest compared with the Northwest, suggesting host trees are more stressed in the Southwest during this critical time for bud growth and larvae feeding. Outbreaks in the Southwest, therefore, benefit from relief from drought in the spring and higher foliage quantity and palatability. In contrast, outbreaks in the wetter Northwest, where hosts are less stressed in spring, benefit from reduced moisture that increases foliage quality. Additional studies are needed to test these ideas with more direct measurements.

Three different moisture metrics were used in this study to present host stress. Multiple previous studies used PDSI as their primary indicator of moisture stress (Swetnam and Lynch 1993, Thomson and Benton 2007, Flower et al. 2014, Flower 2016, Senf et al. 2016). A disadvantage of PDSI is that it does not distinguish between snow (which may stay for months before melting and delivering moisture to host trees) and rain, but instead only considers precipitation. For regions studied here, this issue may be problematic for representing the influences of winter and spring moisture on host trees stress and outbreaks of

WSBW. Summer PDSI may more accurately represent stress conditions during this season since it is less affected by snow than spring and winter. I also considered CWD as another indicator of host tree stress. Unlike PDSI, CWD represents the impact of snow and snowpack melt on soil moisture, which makes it especially useful for regions used in this study. PDSI and CWD analysis showed very similar patterns, but CWD exhibited a slightly stronger drought influence on outbreak initiation. More data, such as local phenology data and snow water equivalent, might be used to identify the time period better and moisture metrics correlate to insect population.

Short-term extreme weather events such as heavy rain or abnormally high fall temperatures may decrease the WSBW population (Fellin and Dewey 1982, Campbell 1993) , yet the influence of those events was not captured by the analysis of this paper. It is possible that my study period was too short such that those events were not present during the study period, or it is possible that the monthly data used here lack the necessary temporal resolution to detect these short-term events.

I selected the climate and insect data sets for use in this study because they were available over broad spatial and temporal scales, yet they are imperfect representations of the processes of interest. The gridded climate data set was developed using various weather data, including station observations. Spatial interpolation was used to fill in gaps, and this interpolation, together with the 4-km spatial resolution, leads to some uncertainty in areas with complex topography, which can have substantial climate variation. The aerial survey insect data were recorded by different surveyors for different forest regions and different years, and this subjectivity may introduce some error. Another limitation of the ADS data is that although these data are from a wide geographic region, they are available for a relatively short period, especially compared with dendrochronological studies. The area covered by surveys also varies every year, which limited regions that can be used for research of continuous events. Areas that are not covered also reduce the accuracy of estimation of insect populations, due to the missing data in some years. This study used defoliation area change as an indicator of insect population dynamics and adjusted the area to include the influence of different severities of defoliation. Damage area represents insect populations at a coarse level, but may also miss critical time periods such as initiation. Actual measurements of insect populations over larger areas and long periods are unavailable.

5. Conclusions

This study analyzed the relationship between drought and recent outbreaks of western spruce budworm and compared patterns in the Northwest US and Southwest US. Similar to past studies, I found that drought facilitates the initiation of WSBW outbreaks in the Northwest. In contrast, in the Southwest, which is on average drier, outbreaks were not associated with drought. No clear relationship exists between insect populations growth rates after an outbreak begins (i.e., during the continuation stage) and moisture metrics in the Northwest, but in the Southwest, increases of insect population may be related to higher spring moisture availability. Thus, other factors are more influential during the continuation stage than climate. Findings were similar to previous studies for a commonly used drought metric, PSDI. I also tested relationships with climatic water deficit and found the same general patterns.

Increases in drought frequency are projected in the coming decades associated with future climate change (Wuebbles et al. 2017). Projected warming will lead to additional stress on plants through enhanced evapotranspiration, even in the absence of reduced precipitation, such that soil moisture is projected to decline in the western US (Wuebbles et al. 2017). Future precipitation is expected to increase in some areas of the western US in some seasons (with more uncertainty than warming), but critically, spring and summer precipitation is projected to decrease (Wuebbles et al. 2017). The findings of this study suggest that we might expect additional severe outbreaks of western spruce budworm in the Northwest in the near future, and this might accelerate succession of coniferous forest types to those better adapted to drier conditions and push the current types to higher latitudes or locations with higher moisture availability. Such information can help inform management of forest types susceptible to defoliation by these insects.

Work Cited

Abatzoglou, J. T., S. Z. Dobrowski, S. A. Parks, and K. C. Hegewisch. 2018. TerraClimate, a high-resolution global dataset of monthly climate and climatic water balance from 1958–2015. Scientific Data **5**:170191.

Brewer, J. W., J. L. Capinera, R. E. Deshon, and M. L. Walmsley. 1985. Influence of Foliar Nitrogen Levels on Survival, Development, and Reproduction of Western Spruce Budworm, Choristoneura Occidentals (Lepidoptera: Tortricidae). The Canadian Entomologist **117**:23-32.

Campbell, R. W. 1993. Population dynamics of the major North American needle-eating budworms.

Daly, C., M. Halbleib, J. I. Smith, W. P. Gibson, M. K. Doggett, G. H. Taylor, J. Curtis, and P. P. Pasteris. 2008. Physiographically sensitive mapping of climatological temperature and precipitation across the conterminous United States. International Journal of Climatology **28**:2031-2064.

Fellin, D. G., and J. E. Dewey. 1982. Western spruce budworm. US Department of Agriculture, Forest Service.

Fick, S. E., and R. J. Hijmans. 2017. WorldClim 2: new 1-km spatial resolution climate surfaces for global land areas. International Journal of Climatology **37**:4302-4315.

Flower, A. 2016. Three Centuries of synchronous forest defoliator outbreaks in western North America. PloS one **11**:e0164737.

Flower, A., D. Gavin, E. Heyerdahl, R. Parsons, and G. Cohn. 2014. Drought-triggered western spruce budworm outbreaks in the interior Pacific Northwest: a multi-century dendrochronological record. Forest Ecology and Management **324**:16-27.

Gower, S. T., K. A. Vogt, and C. C. Grier. 1992. Carbon dynamics of Rocky Mountain Douglas-fir: influence of water and nutrient availability. Ecological Monographs **62**:43-65.

Hard, J. S., S. Tunnock, and R. G. Eder. 1980. Western spruce budworm defoliation trend relative to weather in the Northern Region, 1969-1979. Missoula, Mont.: USDA Forest Service, Northern Region, State & Private Forestry.

Harris, I., P. D. Jones, T. J. Osborn, and D. H. Lister. 2014. Updated high‐resolution grids of monthly climatic observations–the CRU TS3. 10 Dataset. International Journal of Climatology **34**:623-642.

Hijmans, R. J., S. E. Cameron, J. L. Parra, P. G. Jones, and A. Jarvis. 2005. Very high resolution interpolated climate surfaces for global land areas. International Journal of Climatology **25**:1965-1978.

Huberty, A. F., and R. F. Denno. 2004. Plant water stress and its consequences for herbivorous insects: a new synthesis. Ecology **85**:1383-1398.

Kobayashi, S., Y. Ota, Y. Harada, A. Ebita, M. Moriya, H. Onoda, K. Onogi, H. Kamahori, C. Kobayashi, and H. Endo. 2015. The JRA-55 reanalysis: General specifications and basic characteristics. Journal of the Meteorological Society of Japan. Ser. II **93**:5-48.

Mattson, W. J., and R. A. Haack. 1987. The role of drought in outbreaks of plant-eating insects. Bioscience **37**:110-118.

McMillin, J. D., and M. R. Wagner. 1996. Season and intensity of water stress effects on needle toughness of ponderosa pine. Canadian Journal of Forest Research **26**:1166-1173.

Nealis, V. G., and J. Régnière. 2009. Risk of dispersal in western spruce budworm. Agricultural and forest entomology **11**:213-223.

Oyler, J. W., A. Ballantyne, K. Jencso, M. Sweet, and S. W. Running. 2015a. Creating a topoclimatic daily air temperature dataset for the conterminous United States using homogenized station data and remotely sensed land skin temperature. International Journal of Climatology **35**:2258-2279.

Oyler, J. W., S. Z. Dobrowski, A. P. Ballantyne, A. E. Klene, and S. W. Running. 2015b. Artificial amplification of warming trends across the mountains of the western United States. Geophysical research letters **42**:153-161.

Oyler, J. W., S. Z. Dobrowski, Z. A. Holden, and S. W. Running. 2016. Remotely sensed land skin temperature as a spatial predictor of air temperature across the conterminous United States. Journal of Applied Meteorology and Climatology **55**:1441-1457.

Palmer, C. W. 1965. Meteorological drought. US Weather Bureau research paper.

Parks, C. G. 1993. The influence of induced host moisture stress on the growth and development of western spruce budworm and Armillaria ostoyae on grand fir seedlings.

Price, P. W. 1991. The plant vigor hypothesis and herbivore attack. Oikos:244-251.

Ryerson, D. E., T. W. Swetnam, and A. M. Lynch. 2003. A tree-ring reconstruction of western spruce budworm outbreaks in the San Juan Mountains, Colorado, USA. Canadian Journal of Forest Research **33**:1010-1028.

Senf, C., M. A. Wulder, E. M. Campbell, and P. Hostert. 2016. Using Landsat to assess the relationship between spatiotemporal patterns of western spruce budworm outbreaks and regional-scale weather variability. Canadian Journal of Remote Sensing **42**:706-718.

Swetnam, T. W., and A. M. Lynch. 1993. Multicentury, Regional‐Scale Patterns of Western Spruce Budworm Outbreaks. Ecological Monographs **63**:399-424.

Thomson, A., R. Shepherd, J. Harris, and R. Silversides. 1984. Relating weather to outbreaks of western spruce budworm, Choristoneura occidentalis (Lepidoptera: Tortricidae), in British Columbia. The Canadian Entomologist **116**:375-381.

Thomson, A. J., and R. Benton. 2007. A 90-year sea warming trend explains outbreak patterns of western spruce budworm on Vancouver Island. The Forestry Chronicle **83**:867-869.

Turchin, P. 2003. Complex population dynamics: a theoretical/empirical synthesis. Princeton university press.

White, T. t. 1984. The abundance of invertebrate herbivores in relation to the availability of nitrogen in stressed food plants. Oecologia **63**:90-105.

Wuebbles, D., D. Fahey, K. Hibbard, B. Dokken, B. Stewart, and T. Maycock. 2017. Climate Science Special Report: Fourth National Climate Assessment, Volume I. Page 470 Washington, DC.

Appendix A: Using Random Forest to Study the Relationship Between Climate and WSBW Outbreaks

This study attempted to use Random Forest to build a model that can predict the presence or absence of WSBW defoliation base on climate and previous year defoliation conditions. The climate data used in the main thesis was used for the climate data that the ADS data were used to provide previous year defoliation condition. Different climate metrics combinations were created so that climate metrics that are highly correlated with each other will not be used in the same model, in order to find the climate metric with the strongest predictive power. One model was built for each region, which each year as a sample input of the model. For the models that used previous year defoliation area, the previous year defoliation area was too influential for the model that the model prediction was almost the same as the previous year defoliation condition (Figure A.1). The cause of this match might be that the region selected all have defoliation area pattern that is very similar to the previous year. Thus this attempt was not successful. An attempt that only used climate data was also made, but the model result was not very reliable that the estimated out of bag error rate was pretty high, and according to the confusion matrix, those models have very low accuracy for the class that has fewer years (Table A.1). This might be caused by the low number of sample that is available for model construction, and some region has a very unbalanced composition, that only a few years has an absence of defoliation.

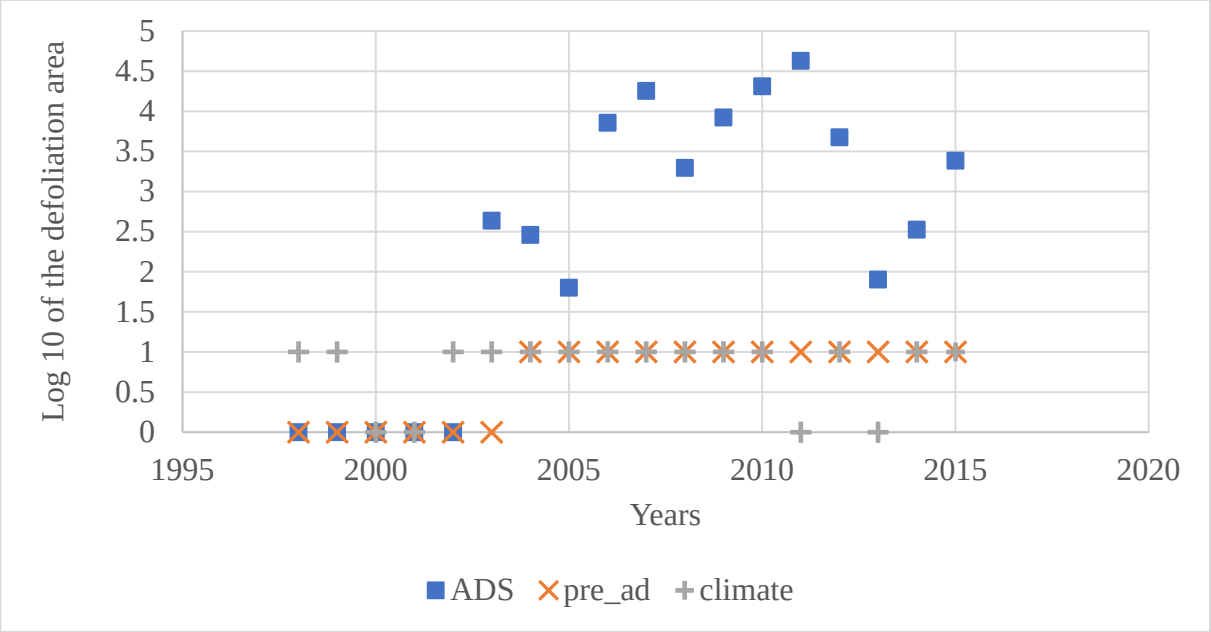

Figure A.1.Example of a model result time series. The ADS series represent the log 10 of defoliation area. The pre_ad series represent the results of models that used previous year defoliation and climate metrics, and the climate series represent the result of the model that only used climate metrics. The result the models were represented using zero and one. Zero indicated the absence of defoliation and one indicated the presence of defoliation.

Table A.1. Example of a model confusion matrix.

OOB estimate of error rate: 33.33%

Confusion matrix:

	absence	presence	Class error
absence	0	5	1
presence	1	12	0.076923

Appendix B: Insect & Disease Detection Survey Attributes Used in This Study.

Insect & Disease Detection Survey attributes used in this study.

Attributes	Brief Description
DCA	Name or code of the damage causal agent, WSBW is 12040.
dmg_type	Name or code of damage type. Code of defoliation is 1.
Pattern	Defoliation pattern code or description. This value describes whether the host species covers more than 50% of the polygon and whether the damage is continuous or patchy.
Severity	Defoliation severity code. Most regions use 1 to represent low severity (equal to or lower than 50% defoliation) and 2 to represent high severity (higher than 50% defoliation).
Acres	Area of the polygon with a unit of acres

Appendix C: SEA Result of Spring Palmer Drought Severity Index

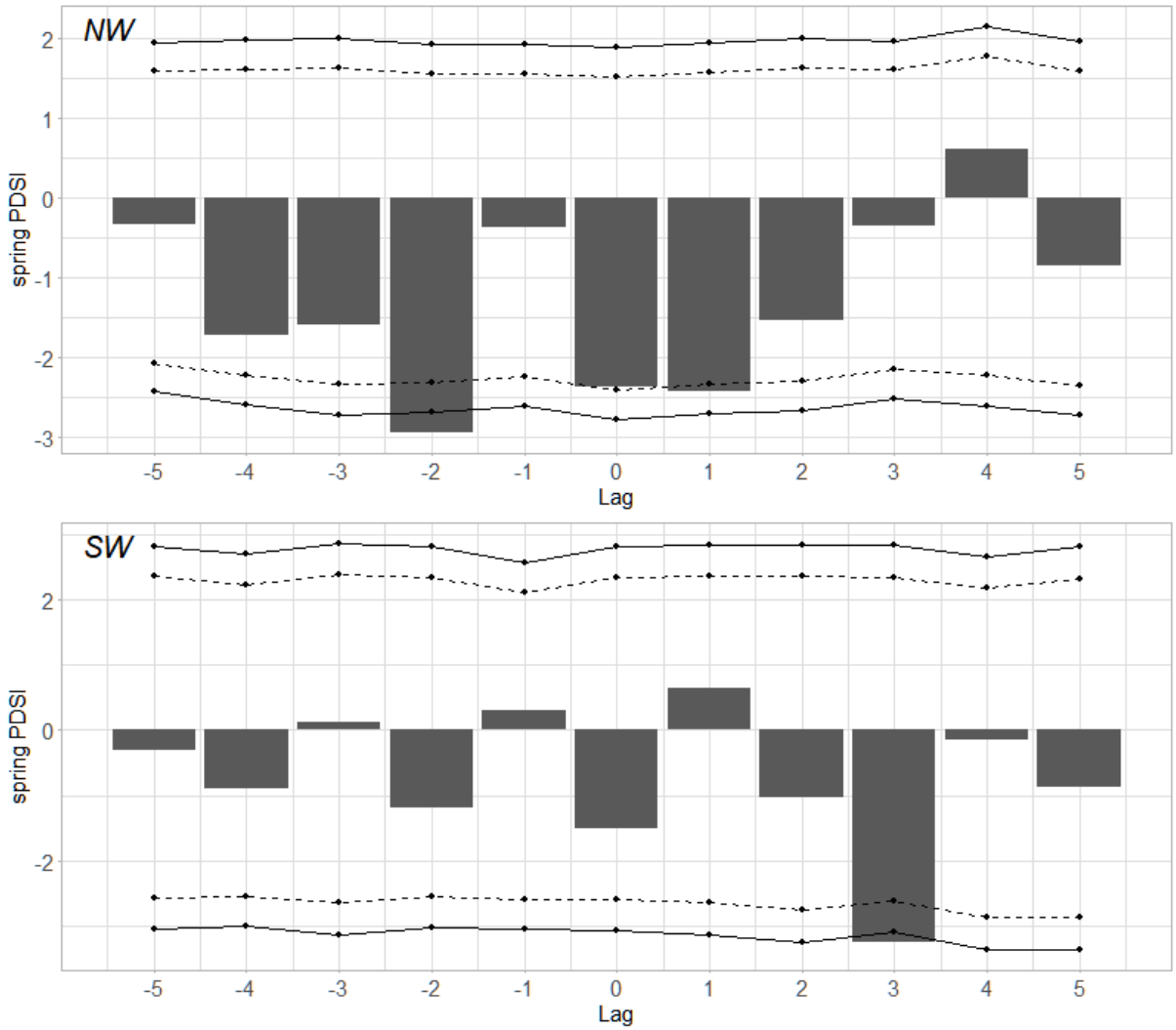

Superposed epoch analysis of spring Palmer Drought Severity Index. Dotted lines indicate the 90% confidence intervals, while the solid lines indicate the 95% confidence intervals.

Appendix D: SEA Result of Fall Palmer Drought Severity Index

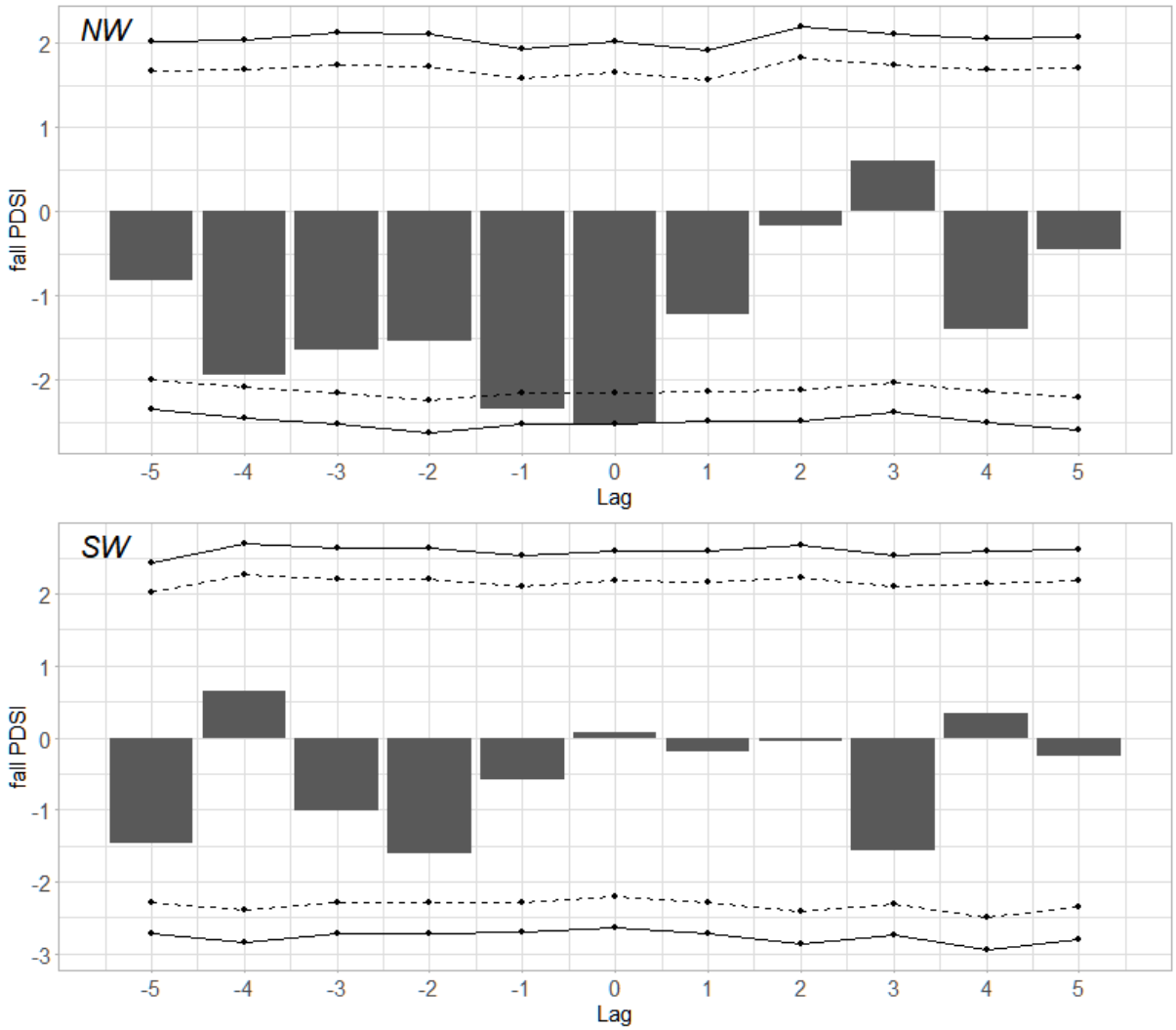

Superposed epoch analysis of fall Palmer Drought Severity Index. Dotted lines indicate the 90% confidence intervals, while the solid lines indicate the 95% confidence intervals.

Appendix E: SEA Result of Winter Palmer Drought Severity Index

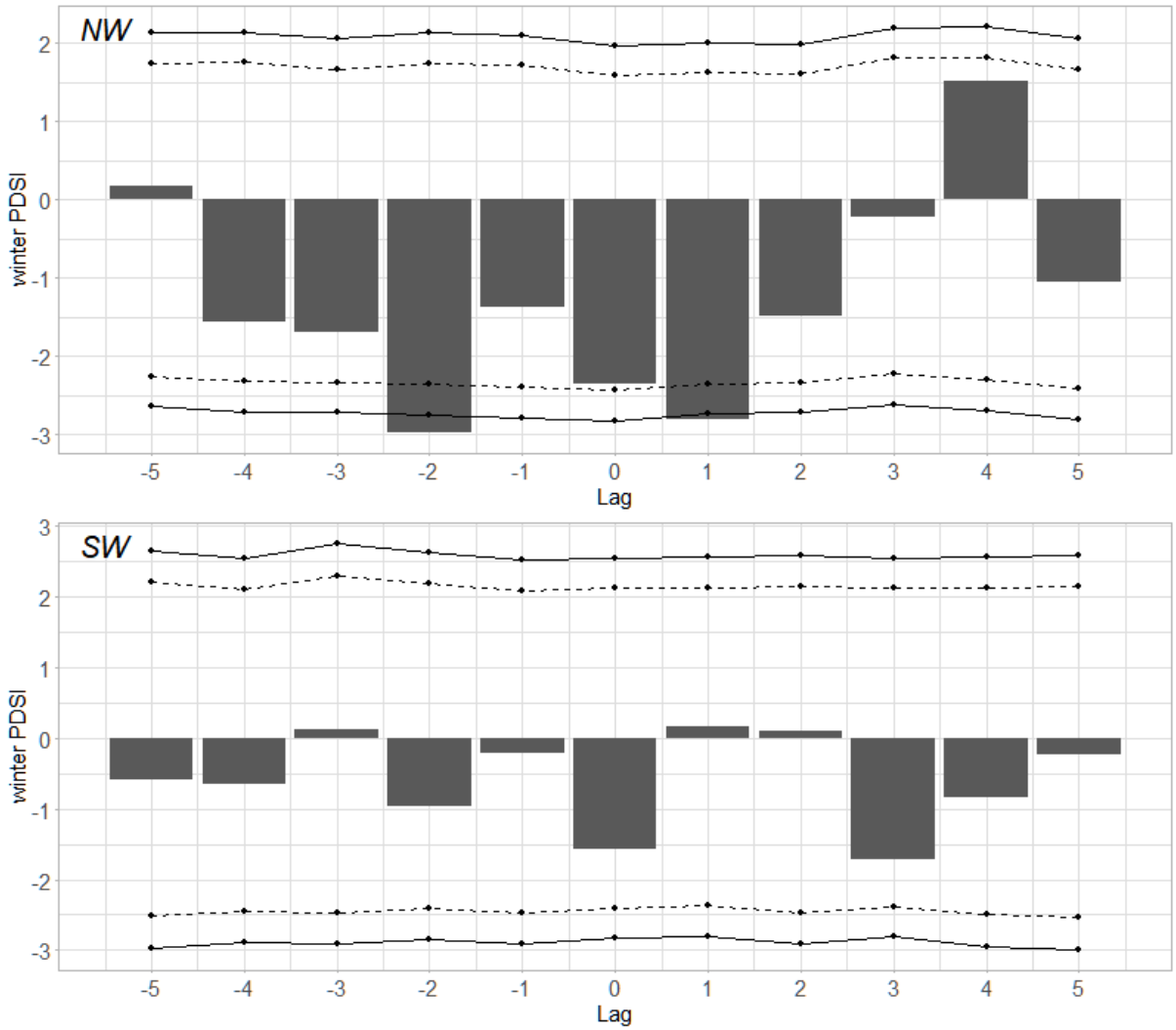

Superposed epoch analysis of winter Palmer Drought Severity Index. Dotted lines indicate the 90% confidence intervals, while the solid lines indicate the 95% confidence intervals.

Appendix F: SEA Result of Water-Year Palmer Drought Severity Index

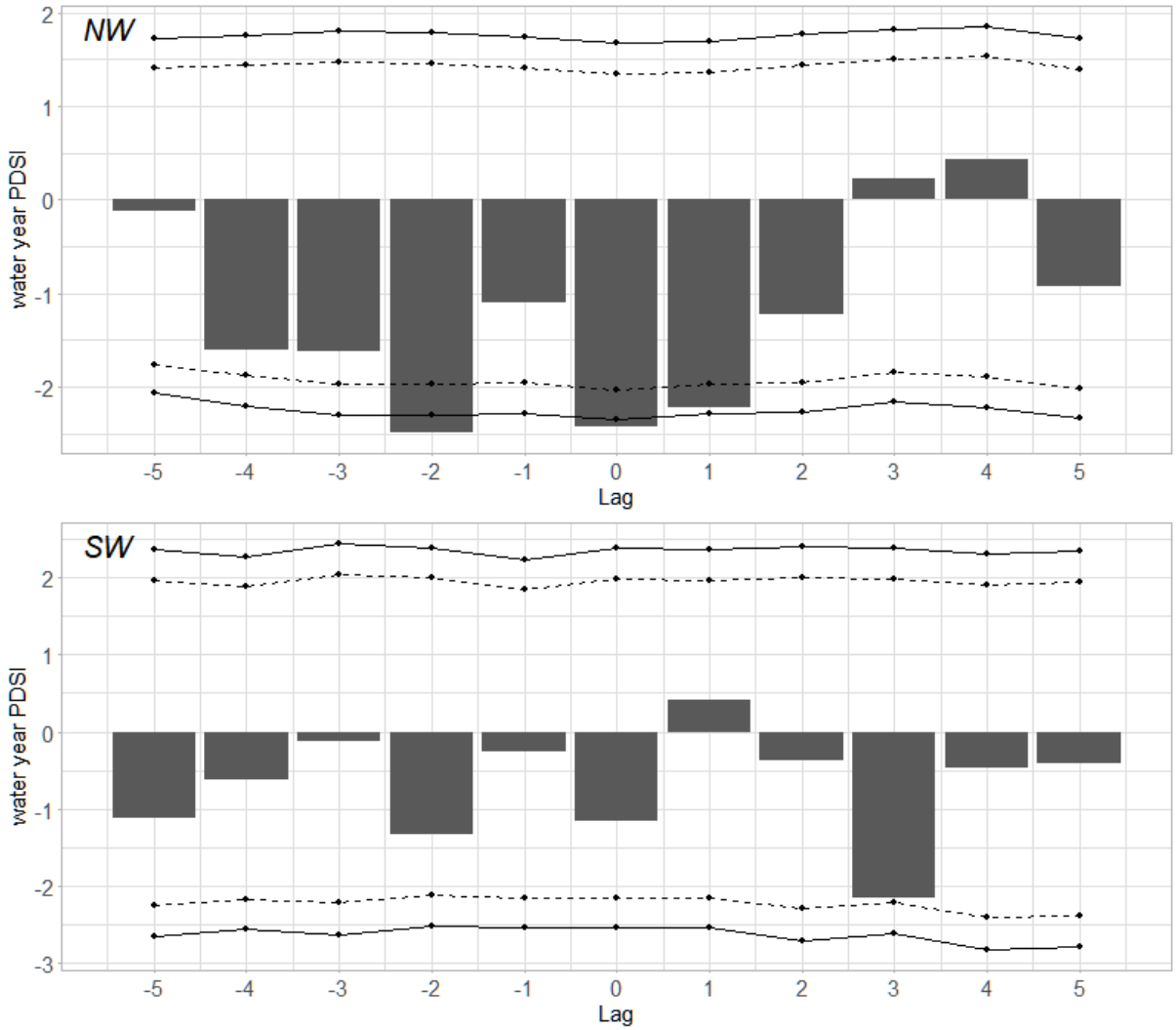

Superposed epoch analysis of water-year Palmer Drought Severity Index. Dotted lines indicate the 90% confidence intervals, while the solid lines indicate the 95% confidence intervals.

Appendix G: Superposed Epoch Analysis Result of Spring Climatic Water Deficit

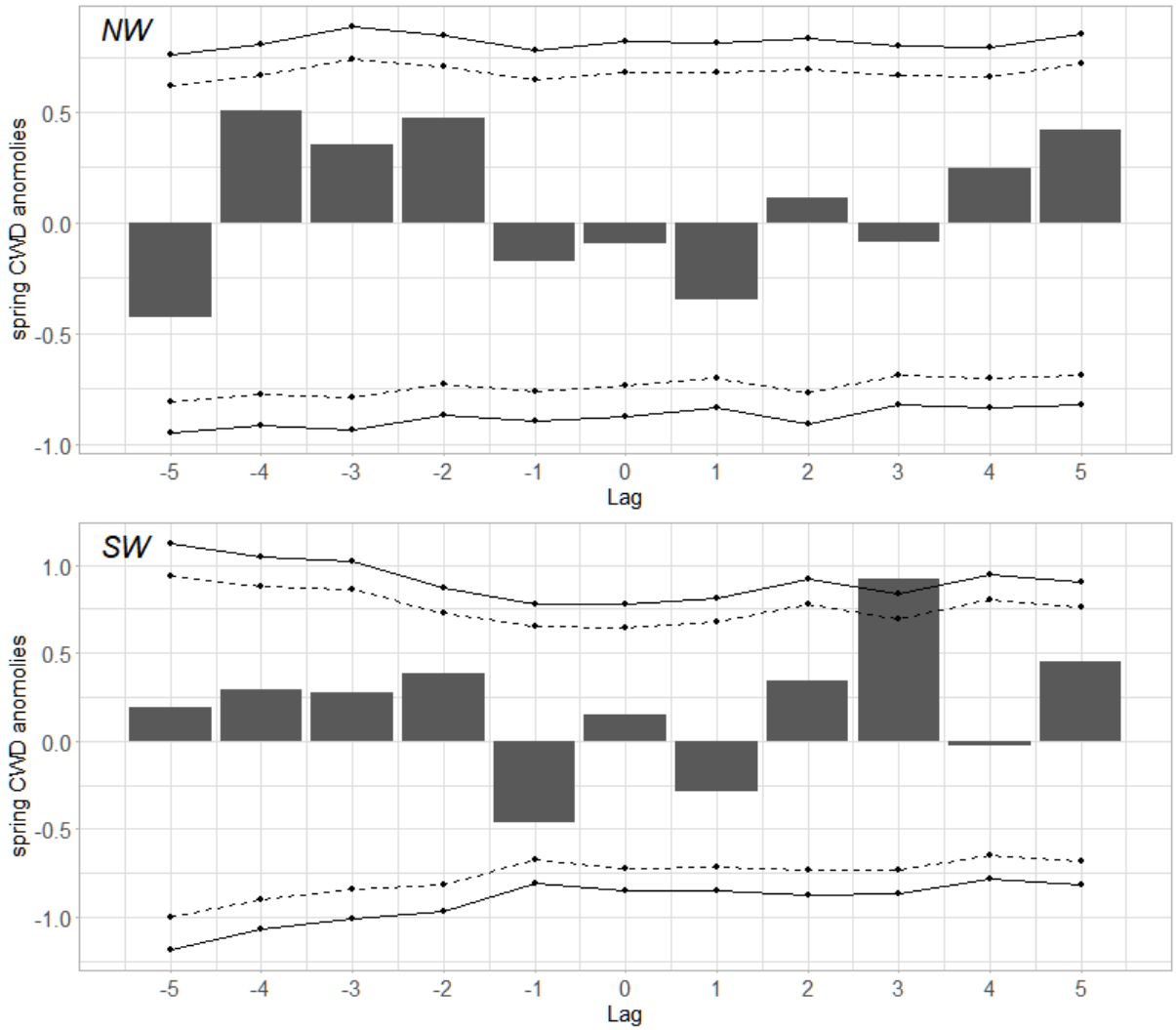

Superposed epoch analysis of spring standardized anomalies of climatic water deficit. Dotted lines indicate the 90% confidence intervals, while the solid lines indicate the 95% confidence intervals.

Appendix H: Superposed Epoch Analysis Result of Fall Climatic Water Deficit

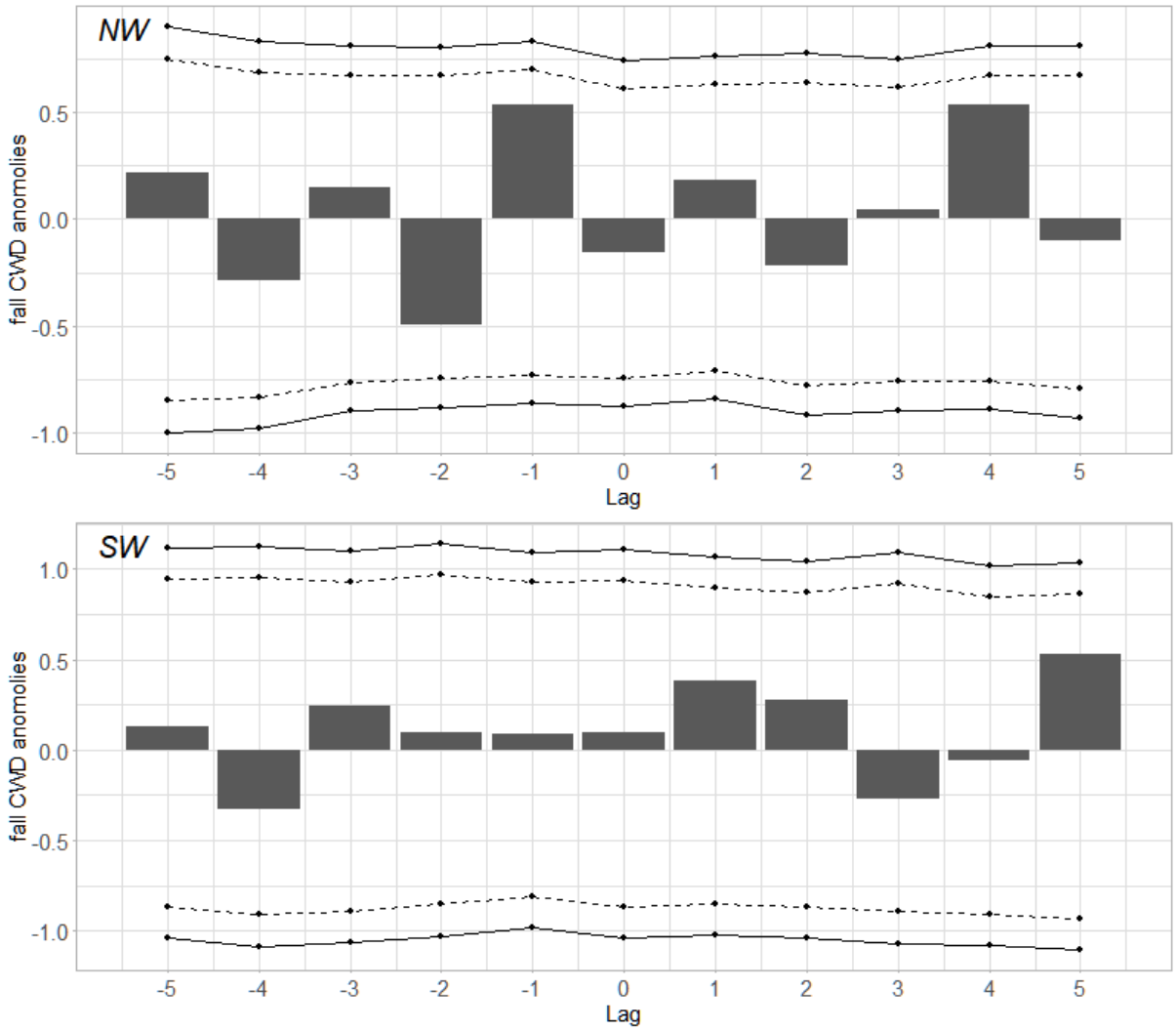

Superposed epoch analysis of fall standardized anomalies of climatic water deficit. Dotted lines indicate the 90% confidence intervals, while the solid lines indicate the 95% confidence intervals.

Appendix I: Superposed Epoch Analysis Result of Winter Climatic Water Deficit

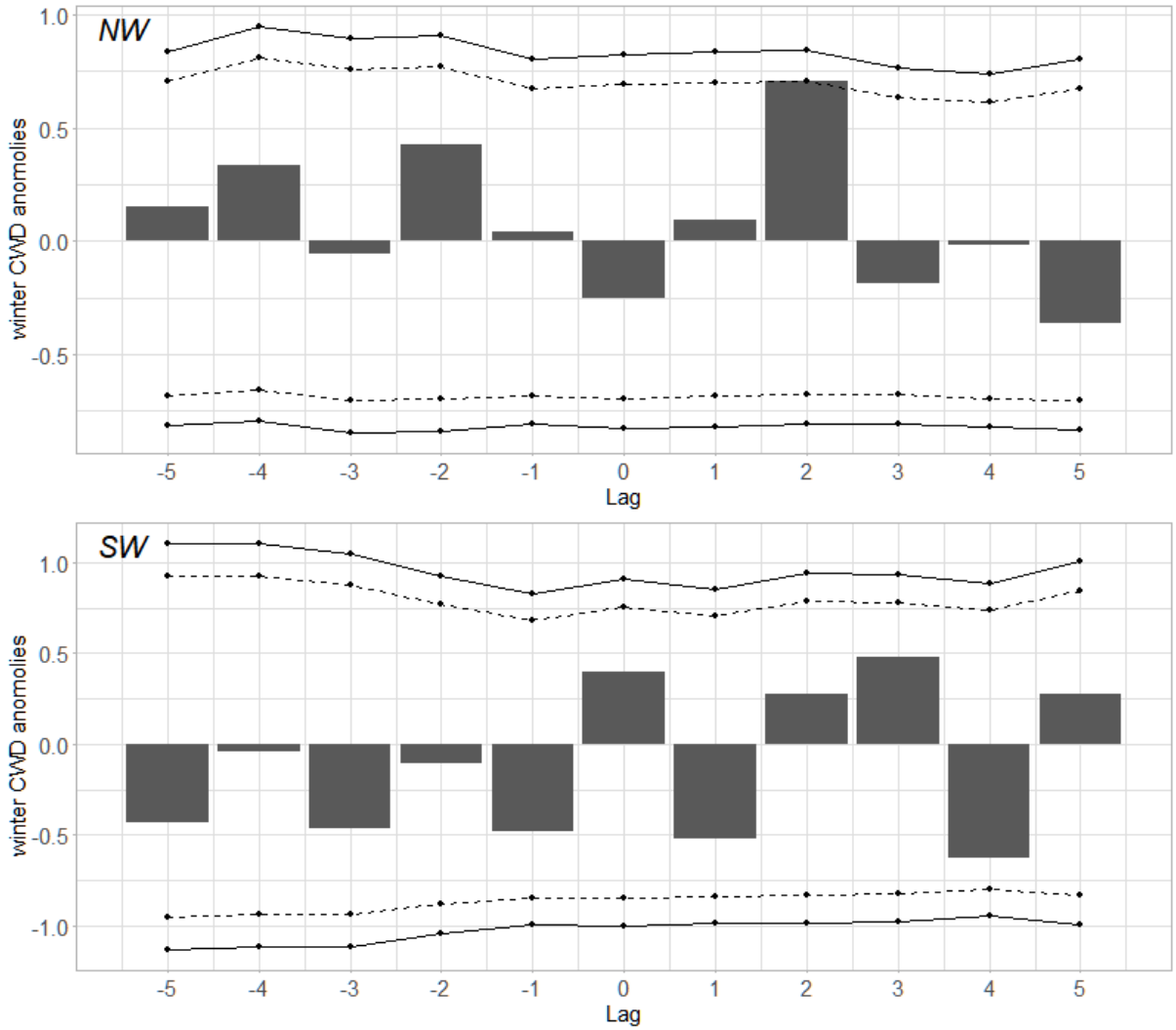

Superposed epoch analysis of winter standardized anomalies of climatic water deficit. Dotted lines indicate the 90% confidence intervals, while the solid lines indicate the 95% confidence intervals.

Appendix J: Superposed Epoch Analysis Result of Water-Year Climatic Water Deficit

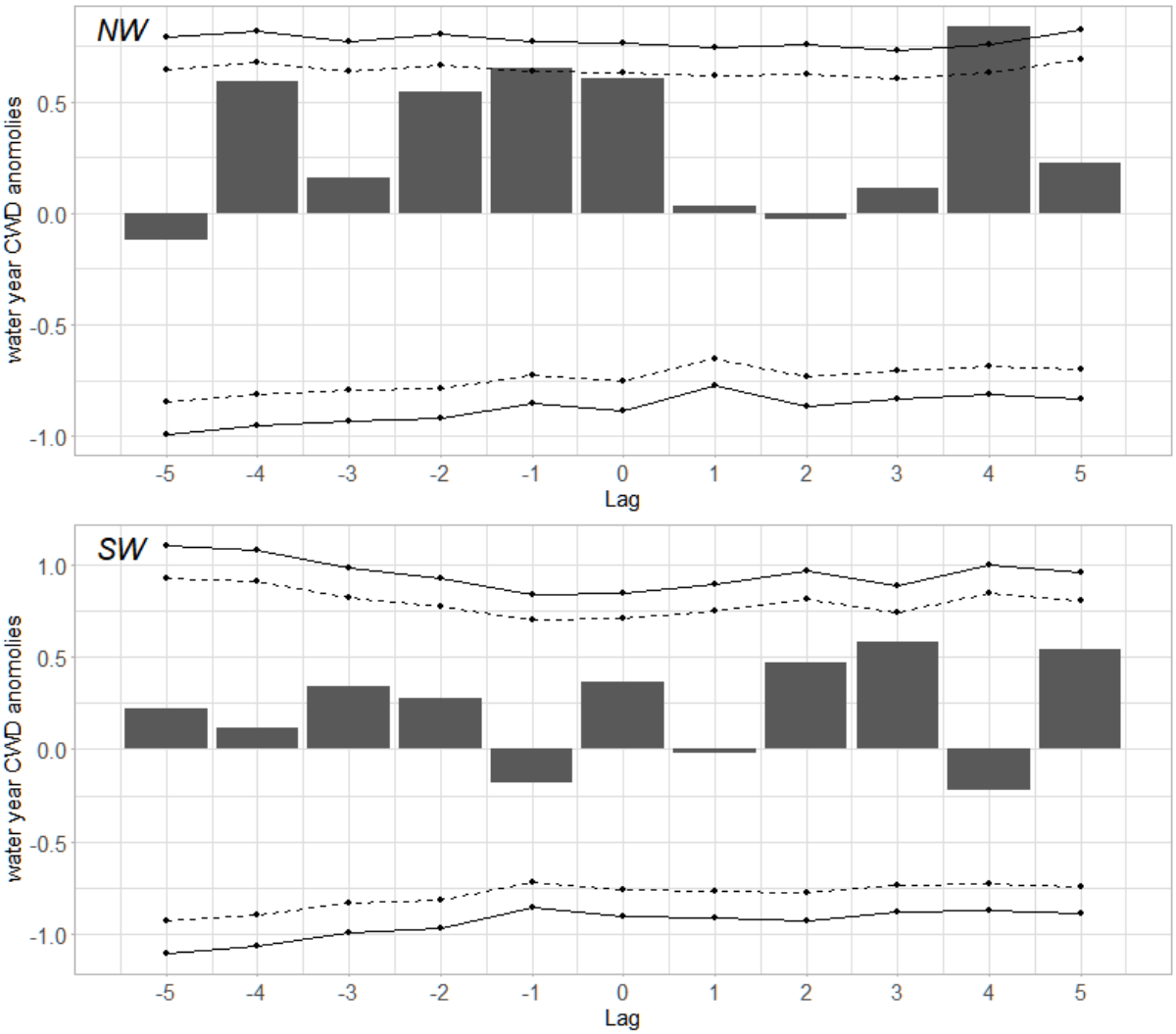

Superposed epoch analysis of water-year standardized anomalies of climatic water deficit. Dotted lines indicate the 90% confidence intervals, while the solid lines indicate the 95% confidence intervals.

Appendix K: Western spruce budworm population growth rate (calculated using adjusted defoliation area from aerial surveys) versus May precipitation

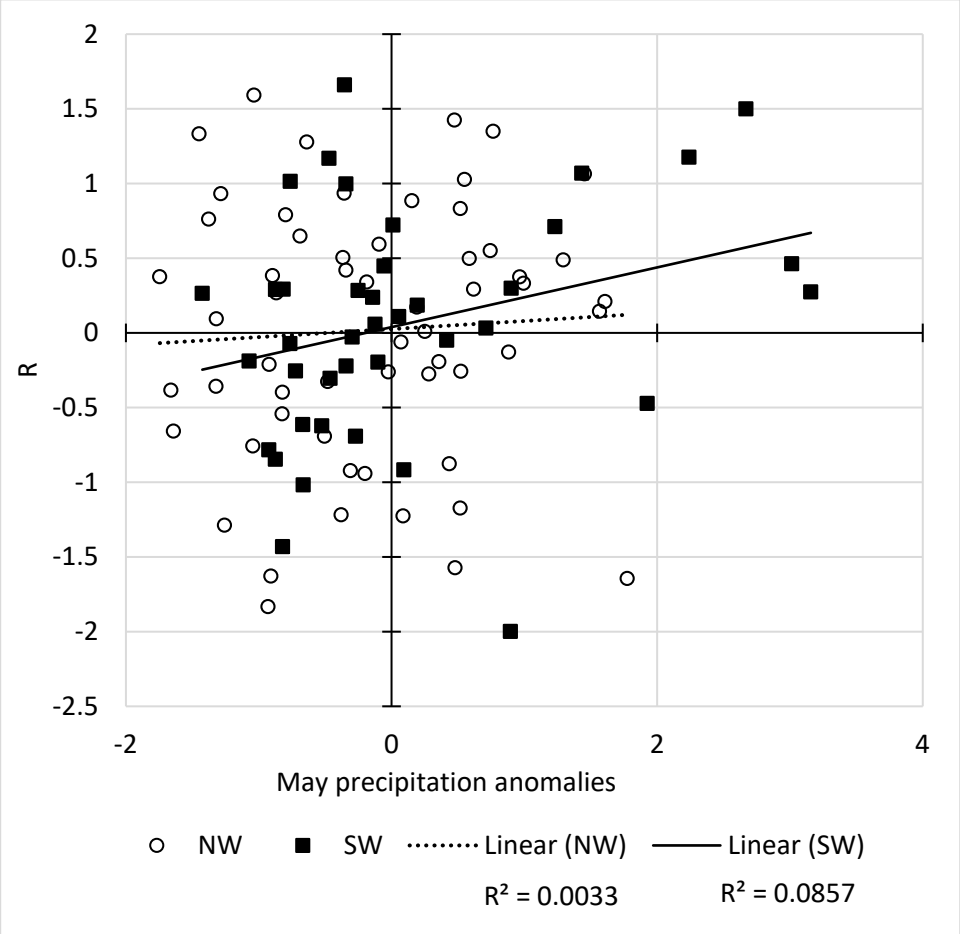

Western spruce budworm population growth rate (calculated using adjusted defoliation area from aerial surveys) versus standardized anomalies of May precipitation . Palmer Drought Severity Index. Solid squares indicate data from years and regions in the Southwest, and hollow circles indicate data from years and regions in the Northwest. The solid line is the trend line of data from Southwest regions, and the dotted line is the trend line of data from Northwest regions

Appendix L: Western spruce budworm population growth rate (calculated using adjusted defoliation area from aerial surveys) versus May Palmer Drought Severity Index

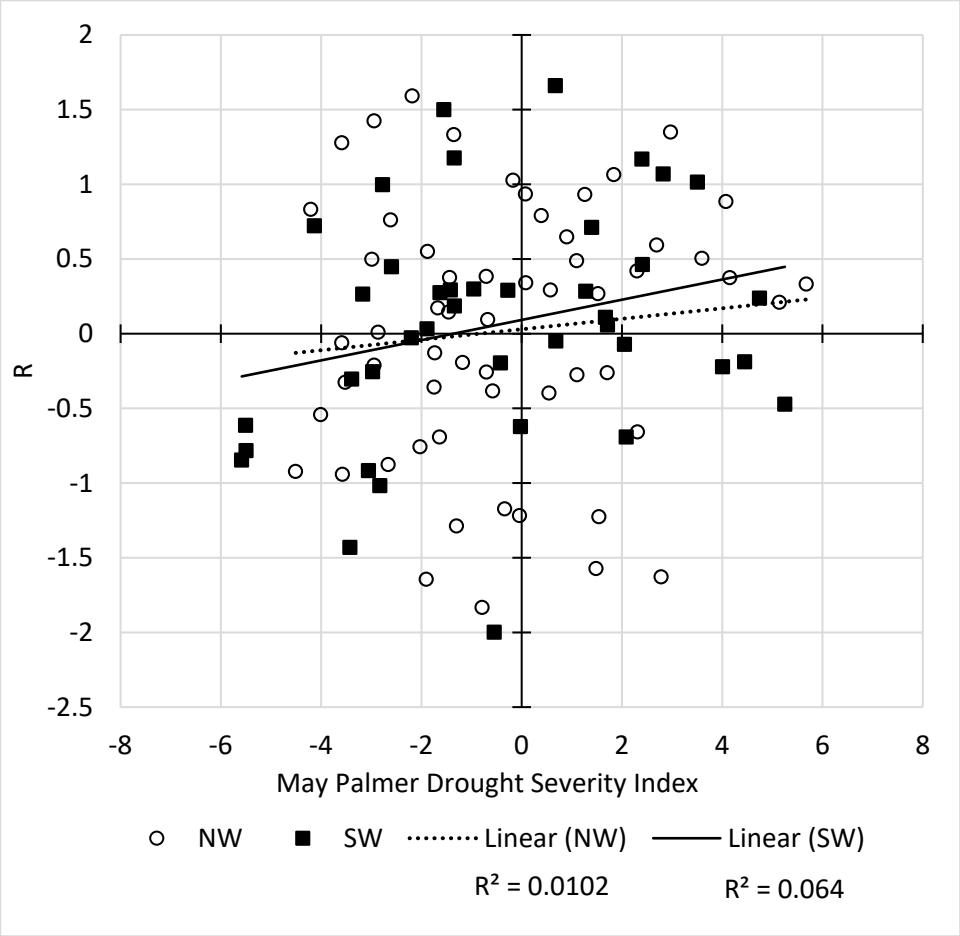

Western spruce budworm population growth rate (calculated using adjusted defoliation area from aerial surveys) versus May Palmer Drought Severity Index. Solid squares indicate data from years and regions in the Southwest, and hollow circles indicate data from years and regions in the Northwest. The solid line is the trend line of data from Southwest regions, and the dotted line is the trend line of data from Northwest regions

Appendix M: Climatic water deficit anomalies of each region

Climatic water deficit anomalies of each region.

	Region 02	Region 03	Region 04	Region 05	Region 06	Region 07	Region 08	Region 10
CWD anomalies of year before initiation	0.09	0.41	1.39	1.67	1.19	0.47	-0.35	0.54
CWD anomalies of initiation year	1.27	1.13	1.09	0.02	0.71	0.67	0.00	-0.83